


RESEARCH ARTICLE

Promoting identification of amyotrophic lateral sclerosis based on label-free plasma spectroscopy

Qi-Jie Zhang¹ , Yang Chen², Xiao-Huan Zou¹, Wei Hu¹, Min-Lu Ye², Qi-Fu Guo¹, Xue-Liang Lin³, Shang-Yuan Feng³ & Ning Wang^{1,4}

¹Department of Neurology and Institute of Neurology, First Affiliated Hospital, Fujian Medical University, Fuzhou, China

²Department of Laboratory Medicine, Fujian Medical University, Fuzhou, China

³Key Laboratory of Optoelectronic Science and Technology for Medicine, Ministry of Education, Fujian Provincial Key Laboratory for Photonics Technology, Fujian Normal University, Fuzhou, China

⁴Fujian Key Laboratory of Molecular Neurology, Fujian Medical University, Fuzhou, China

Correspondence

Ning Wang, Department of Neurology and Institute of Neurology, First Affiliated Hospital, Fujian Medical University, 20 Chazhong Road, Fuzhou, China. 350005. Tel: 086-591-87982772, Fax: 086-591-83375472, E-mail: nwang900@yahoo.com

Shang-Yuan Feng, Key Laboratory of Optoelectronic Science and Technology for Medicine, Ministry of Education, Fujian Provincial Key Laboratory for Photonics Technology, Fujian Normal University, 8 Shangsang Road, Fuzhou, China. 350007. Tel: 086-591-83465373; Fax: 086-591-83465373; E-mail: syfeng@fjnu.edu.cn

Qi-Jie Zhang, Department of Neurology and Institute of Neurology, First Affiliated Hospital, Fujian Medical University, 20 Chazhong Road, Fuzhou, China. 350005. Tel: 086-591-87982772; Fax: 086-591-83375472; E-mail: qijiezhang86@fjmu.edu.cn

Received: 10 August 2020; Revised: 25 August 2020; Accepted: 27 August 2020

Annals of Clinical and Translational Neurology 2020; 7(10): 2010–2018

doi: 10.1002/acn3.51194

Qi-Jie Zhang and Yang Chen contributed equally to this work.

Introduction

Amyotrophic lateral sclerosis (ALS), also known as Lou Gehrig's disease or motor neuron disease (MND), is a chronic and fatal neurodegenerative disease characterized by degeneration of motor neurons in the brain and spinal cord, which subsequently leads to progressive muscle

Abstract

Objective: Amyotrophic lateral sclerosis (ALS) is an adult-onset fatal neurodegenerative disease which lacks identified biological markers. A label-free plasma surface-enhanced Raman spectroscopy (SERS) method was developed to explore a simple and noninvasive test for ALS. **Methods:** ALS patients were enrolled serially and plasma samples were collected at the time of diagnosis prior to the start of ALS treatment. SERS spectra were recorded using a Renishaw micro-Raman system. **Results:** To exclude the interference by varying disease severity, we enrolled three groups of ALS patients, including ALS-1 ($n = 60$; ALSFRS-R ≥ 42 and time interval ≤ 12 months), ALS-2 ($n = 61$; ALSFRS-R < 42 and time interval ≤ 12 months), and ALS-3 ($n = 61$; ALSFRS-R ≥ 38 and time interval > 12 months). The SERS spectra were analyzed using principal component analysis (PCA), which showed that ALS-1, ALS-2, ALS-3, and control groups were separated significantly. Then, decision tree (DT) models and receiver operating characteristic curves were employed and identified that bands at 722 and 739 cm^{-1} , and ratios of 635–722 cm^{-1} and 635–739 cm^{-1} were able to distinguish ALS from controls significantly. Finally, we highlighted six metabolism pathways correlated with ALS, including phenylalanine-tyrosine-tryptophan biosynthesis, aminoacyl-tRNA biosynthesis, phenylalanine metabolism, pantothenate and CoA biosynthesis, porphyrin and chlorophyll metabolism, and pyrimidine metabolism. **Interpretation:** Plasma SERS could be a promising tool for the detection of ALS. The bands at 722 and 739 cm^{-1} , and the ratios of 635–722 cm^{-1} and 635–739 cm^{-1} could serve as potential indicator for ALS.

paralysis and eventual death from respiratory failure within 3–5 years after symptom onset.¹ As the most common type of MND in adults, the worldwide prevalence of ALS was about 4.42 per 100,000 people and the incidence rate is rising year by year.² Until now, no efficacious treatments are available for ALS. The etiology of ALS remains incompletely defined. The majority of ALS cases are sporadic

without apparent family history of the disease, whereas only 5–10% of cases are familial with high genetic heterogeneity. More than 30 genes have been identified in ALS, and among them, the *C9orf72*, *SOD1*, *FUS*, and *TDP-43* are the most common disease-determining genes.^{3–4} Present evidence supports the belief that the development of ALS could be largely attributed to an adverse interplay between genetic and environmental factors, and the disturbances of RNA metabolism, protein degradation, and energy metabolism are the main cellular abnormalities.⁵

Currently, there are no reliable and sensitive biomarkers for ALS. Surface-enhanced Raman spectroscopy (SERS) is a label-free analytical approach for providing fingerprinting type information on macromolecules, such as proteins, nucleic acid, and lipids, and has been widely applied in detecting chemical compound in biofluids, cells, and tissues.^{6–7} In our previous study, we observed that the SERS spectra of ALS patients with short-duration group (≤ 3 years) were significantly different from long-duration group (> 3 years), and the metabolisms of glucose, amino acid, nucleic acid, and antioxidant were highly correlated with disease progression.⁸ Recently, Carlomagno et al. also reported that salivary Raman spectra could be a potential biomarker for ALS in a small sample size of late-stage ALS patients, which provided additional evidence that SERS spectroscopy could be a useful tool for the diagnosis of ALS.⁹ For the time being, no study has been reported to compare the plasma SERS spectra between ALS patients and healthy controls, and the ALS-relevant SERS bands have not been identified. We analyzed the plasma-nanoparticle complexes-based SERS features in ALS patients and healthy controls, aiming to search for specific SERS markers that could serve as potential indicator of ALS.

Methods

Subjects

The ALS patients were enrolled serially from the Department of Neurology, First Affiliated Hospital of Fujian Medical University from January 2015 to December 2018. The patients who had a known family history of ALS were defined as familial ALS. All cases were diagnosed as definite, probable, or possible ALS according to El Escorial criteria, and the diagnosis was confirmed by at least two professional neurologists.¹⁰ The healthy controls were those who have not suffered from neurological disease and have not shown a known family history of ALS, and those who have not shown any neurological symptoms when the blood samples were collected. This study was approved by the Ethics Board of First Affiliated Hospital of Fujian Medical University. Written informed consent was obtained from each participant. The peripheral vein blood sample was

drawn after 12 h of overnight fasting. Plasma was separated out after centrifuging for 10 min at 1000 g, and frozen at -80°C . Patients who refused to participate or the plasma sample was not available were excluded.

Preparation of plasma-nanoparticle complexes

Plasma samples were subsequently mixed with silver colloidal substrate to prepare plasma-nanoparticle complexes. These complexes were prepared based on deoxidizing method using hydroxylamine hydrochloride and silver nitrate that is deemed to acquire Ag nanoparticles.¹¹ For nanoparticle preparation, 0.1 mol/L sodium hydroxide solution and 6×10^{-2} mol/L hydroxylamine hydrochloride solution were mixed under ratio of 9 mL: 10 mL. Then, the mixture was moved rapidly to 180 mL of 1.11×10^{-3} mol/L silver nitrate aqueous solution, and gently shaken until a homogenous state with final colloid of milky gray color. Finally, the silver colloidal solution needs to be concentrated by centrifugation at 6950 g for 10 min, discarding a portion of the supernatant. The plasma sample and silver colloidal solution were mixed under volume of 1:1. A pipette tip was used to make the plasma-nanoparticle complexes as homogenous as possible, and the final mixture sample was transferred onto a rectangle aluminum plate for further SERS measurements.

SERS measurements

The protocol for SERS experiment was previously described.⁸ The SERS spectra were recorded using an InVia Micro-Raman system (Renishaw Corporation, Gloucestershire, London, England) under 785-nm diode laser excitation with the Raman shift range from 300 cm^{-1} to 1800 cm^{-1} . The spectra were collected in the backscattering geometry by a microscope equipped with a $20\times$ objective lens, with a spectral resolution of 1 cm^{-1} and an exposure time of 10 sec.

Data processing and pattern recognition

An automated algorithm described previously was used to remove the autofluorescence background and then extract the pure SERS spectra.¹² The SERS spectra were then normalized according to the area under the curve (AUC). The whole SERS spectra of ALS patients and controls were analyzed by principal component analysis (PCA). The significant bands were then identified using the classification and regression trees (CRT) algorithm. The receiver operating characteristic (ROC) curves were drawn by the Prism software (GraphPad Prism v6.0). The map of biochemical pathways based on the screened important

bands was drawn by the MetaboAnalyst-based tool, with custom networks defined by the Kyoto Encyclopedia of Genes and Genomes (KEGG) online database. The statistical analysis was carried out by SPSS v.19.0 software (IBM Corporation, Chicago, IL, USA). $P < 0.05$ (two-tailed) was considered as statistically significant.

Results

Clinical features and subgroups of ALS patients

Given the plasma SERS spectra might be affected by varying disease severity and treatment or lifestyle change after diagnosis of ALS, we collected the plasma sample at the time of diagnosis prior to the start of ALS treatment. We also assessed the disease severity using ALSFRS-R score, and calculated the time interval between symptom onset and plasma collection. In total, 238 ALS patients were serially enrolled from January 2015 to December 2018. The mean ALSFRS-R score was 38 ± 7 , and the median score was 40 (tertile range: 37–42). The median interval between symptom onset and plasma collection was 12 months. We then divided the ALS cases into three subgroups based on the ALSFRS-R score and time interval between symptom onset and plasma collection. The group 1 (ALS-1) included the cases whose ALSFRS-R score was more than 42 and time interval less than 12 months. The group 2 (ALS-2) included the cases whose ALSFRS-R score was less than 42 and time interval less than 12 months. The group 3 (ALS-3) included the cases whose ALSFRS-R score was more than 38 and time interval more than 12 months. Among the ALS groups, there were 12 familial cases and the remaining 170 cases were sporadic. We also enrolled 60 healthy controls who did not suffer from neurological disease and did not show any neurological symptoms when the blood sample was collected. No significant differences

were observed with respect to gender ($P = 0.059$) and the age of plasma collection ($P = 0.066$) between ALS and control groups. The detailed characteristics are shown in Table 1.

Plasma SERS spectral features for ALS patients and controls

We recorded the SERS spectra of plasma samples from three groups of ALS patients ($n = 182$) and healthy controls ($n = 60$) under the same instrumentation setup. The Raman signals were amplified using silver colloidal nanoparticles (Ag NPs) (Fig. 1A). Based on the raw data of whole SERS spectra, we obtained the mean spectra for ALS-1, ALS-2, ALS-3, and control group (Fig. 1B). We could observe several prominent SERS bands obviously, which were then assigned to specific compounds according to previous studies (Table 2).^{13–15} From Figure 1B, similar primary SERS peaks were observed in both ALS and normal blood plasmas, with the strongest signals at 493, 635, 1198, and 1648 cm^{-1} . The normalized intensities of SERS bands at 493, 587, 681, 722, 739, 808, 1001, 1198, 1385, 1450, 1567, and 1618 cm^{-1} were stronger for ALS patients than that for healthy controls, while the SERS bands at 529, 635, 1068, 1252, and 1507 cm^{-1} were stronger in healthy control samples.

Identification of specific SERS bands for ALS

Could the different SERS spectra be able to distinguish ALS cases from normal controls? To address this question, firstly, we entered the data from the whole SERS spectra into SPSS software for PCA analysis. As shown in Figure 2A–C, it indicated that ALS-1 and control, ALS-2 and control, and ALS-3 and control were clearly separated, highlighting that there are significant differences in plasma samples between ALS patients and controls. Secondly, we constructed decision tree (DT) classification models for ALS-1 and control, ALS-2 and control, and

Table 1. The characteristics of the ALS patients and controls

Variables	Groups			
	ALS-1 ($n = 60$)	ALS-2 ($n = 61$)	ALS-3 ($n = 61$)	Control ($n = 60$)
Gender, male:female	40:20	37:24	39:22	30:30
Age of sample collection, mean (SD), y	52.9 (10.5)	57.2 (10.8)	52.4 (10.2)	51.2 (10.7)
Site of onset, bulbar:upper:lower limb (n)	16:28:16	13:27:21	11:32:18	–
Time interval between symptom onset and sample collection, median (IQR), mo	6 (5–9)	9 (6–11)	20 (14.5–30)	–
ALSFRS-R score at sample collection, median (IQR)	45 (43–46)	38 (34–40)	41 (39–44)	–

ALS, amyotrophic lateral sclerosis; ALSFRS-R, Amyotrophic Lateral Sclerosis Functional Rating Scale–Revised; ALS-1, ALS group 1; ALS-2, ALS group 2; ALS-3, ALS group 3; SD, standard deviation; IQR, Interquartile range.

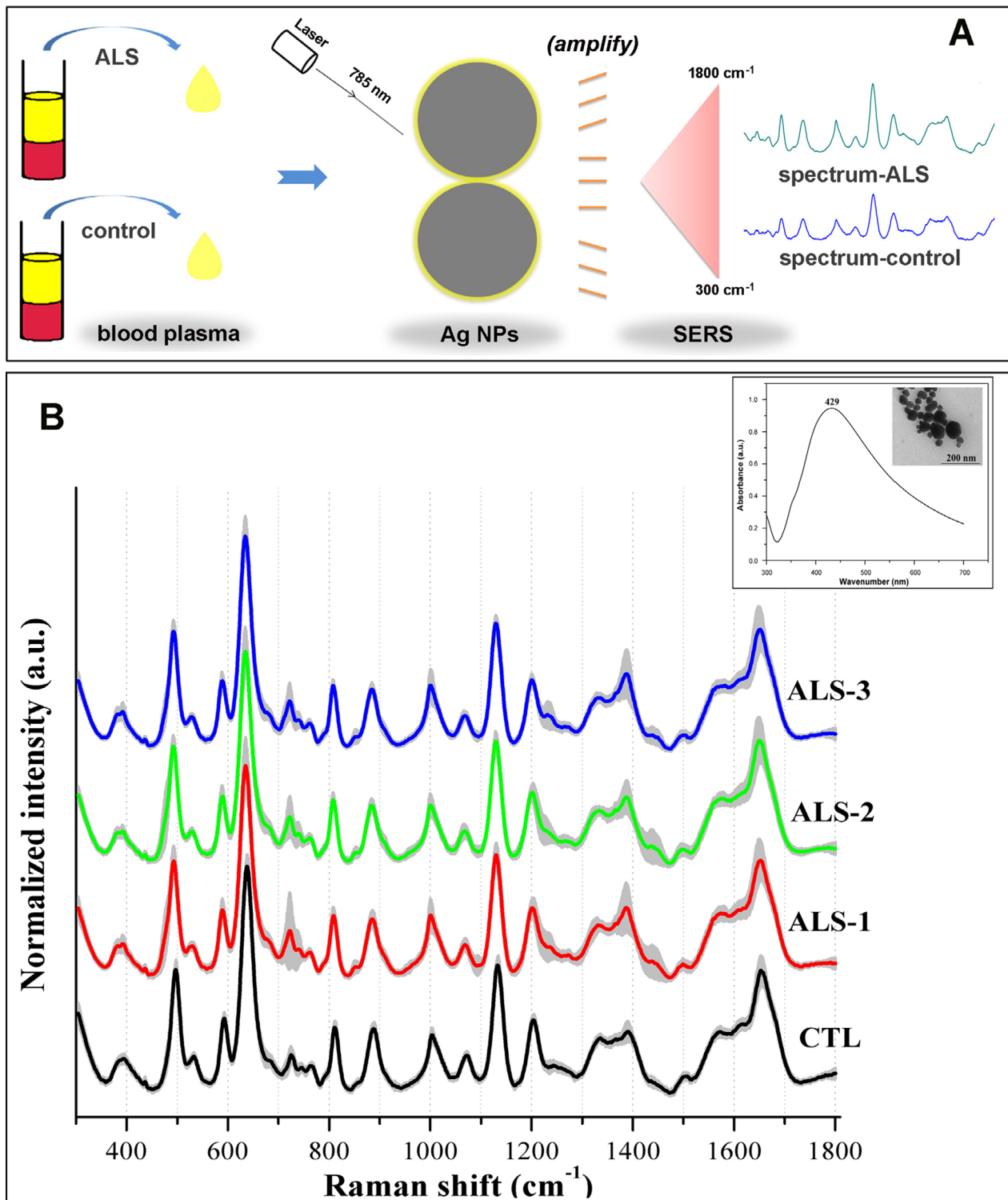


Figure 1. (A) Schematic illustration of blood plasma SERS analysis. (B) The absorption curve and micrograph of silver colloidal nanoparticles (Ag NPs). The absorption maximum was located at 429 nm. The mean blood plasma spectrum for ALS-1 (red line, $n = 60$), ALS-2 (green line, $n = 61$), ALS-3 (blue line, $n = 61$), and control group (black line, $n = 60$). The shaded areas represent the SDs of the means. ALS, amyotrophic lateral sclerosis. CTL, control.

Table 2. The band position, major components, and vibrational mode of SERS from blood plasma

Band position (cm ⁻¹)	Major components	Vibrational mode
493	Arginine, glycogen	S-S stretching
529	Cholesterol ester	
587	Ascorbic acid, amide-VI	
635	Tyrosine, lactose	C-S stretching
681	Guanine	ring breathing
722	Adenine, coenzyme A	C-H bending
739	Thymine, uracil	
760	Tryptophan	Pyrimidine ring breathing
808	Phosphodiester bands in RNA, L-Serine	C-C-O stretching
882	Glutathione, D-(C)-galactosamine	C-O-H bending
1001	Phenylalanine	C-C stretching
1068	Collagen	C-N stretching
1130	D-mannose	C-N stretching
1198	L-tryptophan, phenylalanine	Ring vibration
1252	Adenine, amide III	
1275	Amide III	
1322	Guanine	
1385		C-H rocking
1450	Protein and lipids	C-H deformation
1507	Adenine	
1567	Myeloperoxidase (MPO), cytochrome, Haem	C-C stretching (conjugated)
1618	Tyrosine, tryptophan	C = C stretching
1648	Amide I	C = O stretching

ALS-3 and control, respectively. The importance of different SERS bands is shown in Figure 2D–F. In different DT models, the important bands and their ranks were varying; however, several similar SERS bands were identified, including bands at 493, 587, 635, 722, 739, 1450, and 1507 cm⁻¹. Thirdly, we evaluated the predictive performance of each SERS band by ROC curve. The normalized intensity distributions and ROC curves of bands at 493, 529, 587, 635, 681, 722, 739, 760, 808, 882, 1001, 1068, 1130, 1198, 1252, 1275, 1322, 1385, 1450, 1507, 1567, 1618, and 1648 cm⁻¹ are shown in Figure S1–S6. Compared with other SERS bands, band of 722 and 739 cm⁻¹ possessed the greatest AUC (Fig. 3A–B). For band of 722 cm⁻¹, the AUC for ALS-1, ALS-2, and ALS-3 was 0.80 (0.72–0.88), 0.85 (0.78–0.92), and 0.85 (0.77–0.92), respectively. For band of 739 cm⁻¹, the AUC for ALS-1, ALS-2, and ALS-3 was 0.73 (0.64–0.83), 0.78 (0.69–0.87), and 0.78 (0.70–0.87), respectively. Fourthly, combined with the results of difference spectra, CRT, and ROC curves, we picked out the bands with more intense in the control group, and the bands with more intense in the ALS groups. Then, we calculated their ratios, and drew

the ROC curves (Fig. S7). The ratio of 635–722 cm⁻¹ and ratio of 635–739 cm⁻¹ possessed the greatest AUC (Fig. 3C–D). For ratio of 635–722 cm⁻¹, the AUC for ALS-1, ALS-2, and ALS-3 was 0.81 (0.73–0.89), 0.86 (0.80–0.93), and 0.86 (0.79–0.93), respectively. For ratio of 635–739 cm⁻¹, the AUC for ALS-1, ALS-2, and ALS-3 was 0.74 (0.65–0.83), 0.79 (0.70–0.87), and 0.80 (0.71–0.88), respectively.

Metabolic pathway and network analysis for ALS

Finally, to explore the ALS disease-related pathway, we performed the pathway analysis with the help of KEGG online database. The important SERS bands were selected based on the CRT results. The ALS disease-related pathways in ALS-1, ALS-2, and ALS-3 groups are shown in Figure 4. There were six main pathways associated with ALS among these three groups, including phenylalanine-tyrosine-tryptophan biosynthesis, aminoacyl-tRNA biosynthesis, phenylalanine metabolism, pantothenate and CoA biosynthesis, porphyrin and chlorophyll metabolism, and pyrimidine metabolism. Furthermore, based on the compounds assigned to SERS bands at 493, 529, 587, 681, 722, 739, and 1507 cm⁻¹, we drew the disease-related metabolic network, which mainly indicated the involvement of DNA/RNA metabolism and energy metabolism (Fig. S8).

Discussion

ALS is an adult-onset and fatal motor neuron degenerative disease, clinically characterized by progressive muscle weakness and atrophy. Pathophysiological mechanisms that contribute to motor neuron degeneration are complicated, including dysfunction of RNA metabolism, DNA damage, toxic protein aggregation, glutamate excitotoxicity, generation of free radicals, disrupted axonal transport, mitochondrial dysfunction, inflammation, apoptosis, and autophagy.^{16–18} A major obstacle has been the lack of reliable and sensitive biomarker. SERS, which is developed based on the routine Raman spectroscopy (RS), has overcome the major obstacle of RS and could largely enhance the Raman signals and suppress the autofluorescence.^{6,19} SERS spectra of plasma could provide abundant information on macromolecules, and there were several primary bands in SERS spectrum, which were assigned to specific compounds based on Raman shift and vibrational mode, such as amino acids, nucleic acids, and lipids. In the present study, we analyzed the SERS spectra features in ALS patients and healthy controls. A positive result was obtained using PCA analysis, which suggested that there were inherent differences in blood plasma between ALS patients and healthy controls.

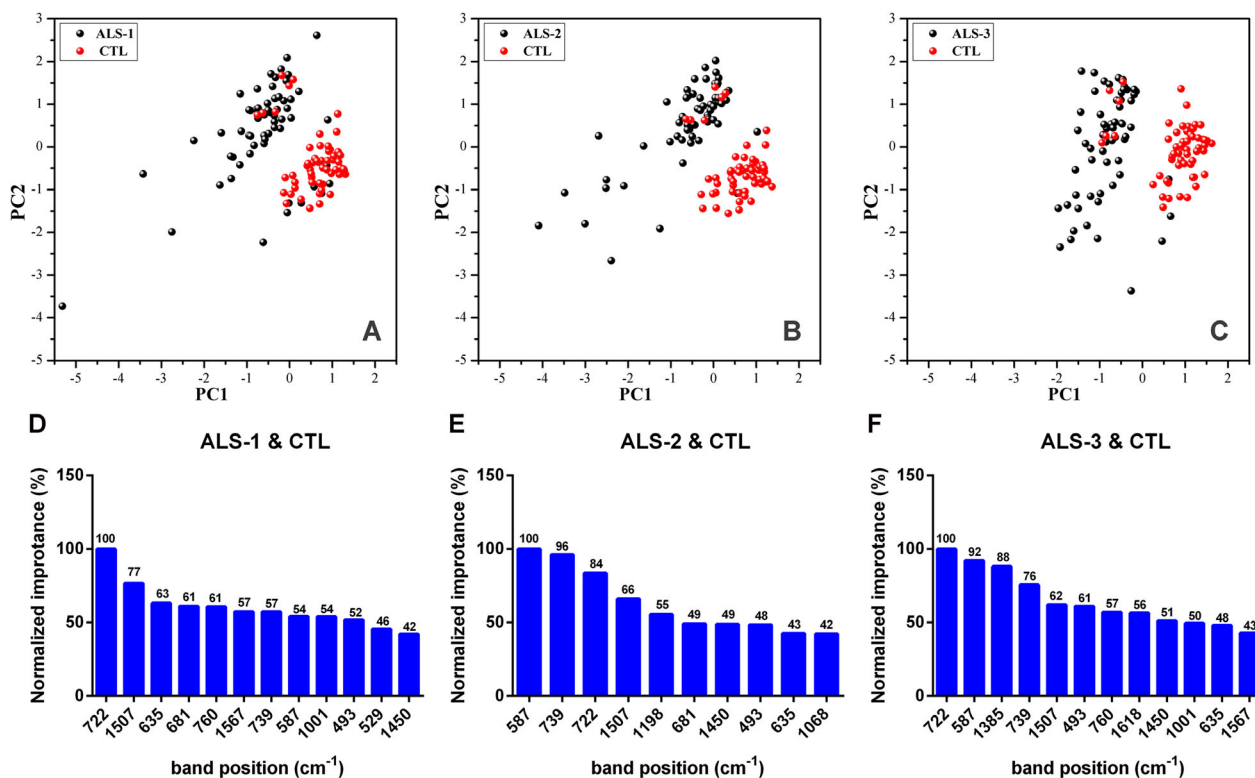


Figure 2. Plots of PC1 versus PC2 for the ALS-1 and control group (A), ALS-2 and control group (B), and ALS-3 and control group (C). The rank and importance of SERS bands in the CRT model between ALS-1 and control group (D), ALS-2 and control group (E), and ALS-3 and control group (F). The length of each bar indicates the quantified importance.

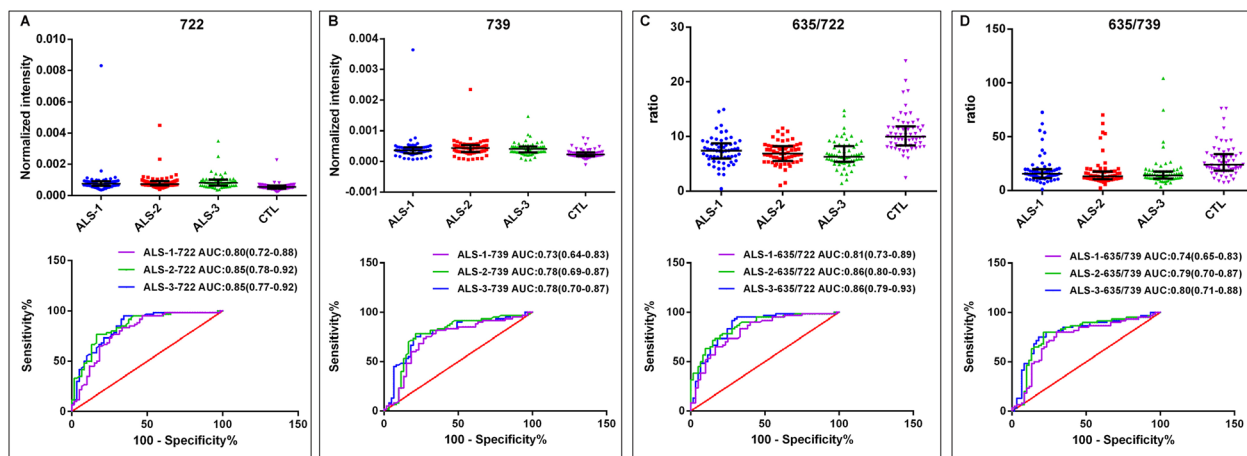


Figure 3. The intensity distribution and ROC curves for ALS-1, ALS-2, and ALS-3 of band at 722 cm⁻¹ (A), 739 cm⁻¹ (B), ratio of 635 cm⁻¹ to 722 cm⁻¹ (C), and ratio of 635–739 cm⁻¹ (D). The intensity distribution was expressed as the median with interquartile range.

The different intensity of SERS bands, in a certain extent, could reflect molecular and cellular changes correlated with development of ALS. Combined with the results of CRT, intensity distributions, and ROC curves, several important SERS bands were identified between

ALS cases and healthy controls, especially the band of 722 and 739 cm⁻¹. The band at 722 cm⁻¹ due to the C-H bending of adenine and coenzyme A exhibited greater intensity in ALS group. The band at 739 cm⁻¹ that corresponds to thymine and uracil also showed higher signal

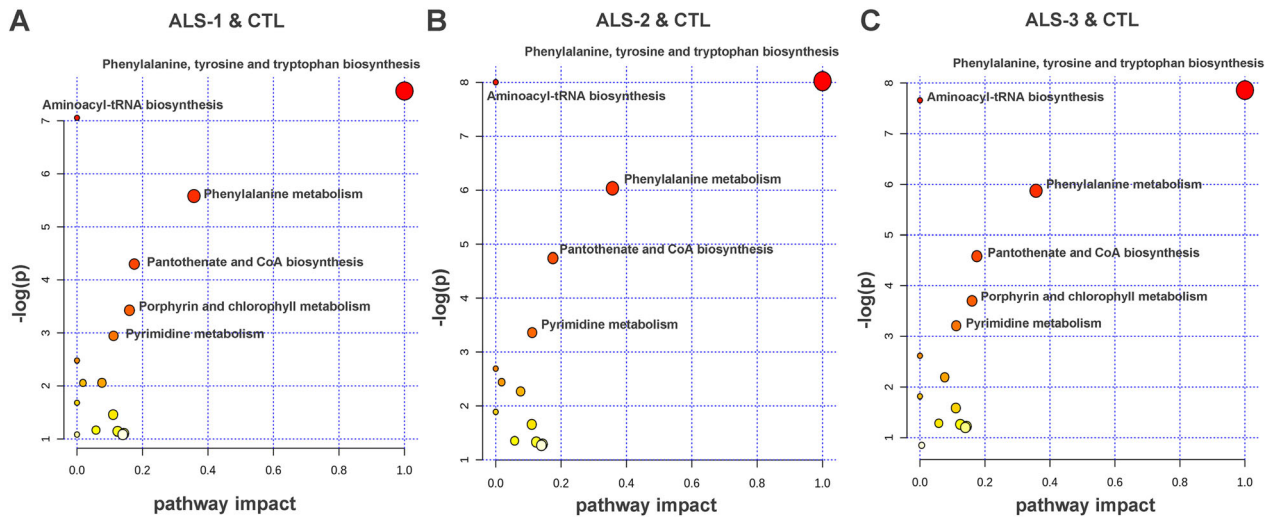


Figure 4. Map of biochemical pathways correlating with ALS-1 and control (A), ALS-2 and control (B), and ALS-3 and control (C). Each circle represents a metabolic pathway. The size of the circle represents the pathway impact value. The color saturation in the circle represents the P value. P values were calculated from pathway enrichment analysis and topology analysis.

in ALS patients. It indicated that there were high levels of DNA or RNA bases in the blood plasma of ALS patients, and the reason remains largely unknown. Abnormalities in DNA repair, or named DNA damage, are implicated in the mechanisms of aging, cancers, and neurological diseases.²⁰ Kim et al. also observed that single-stranded DNA significantly accumulated in brain and spinal motor neurons in ALS patients.²¹ Besides, more and more RNA-binding protein (RBP) genes were identified to cause or increase the risk for ALS, such as *TDP-43*, *FUS*, *hnRNPA1*, *ATXN2* etc. The RBP genes play crucial roles in RNA metabolism, including transcription, RNA splicing, mRNA transport, nuclear export, sequestration, and degradation.²² We propose that the concentrations of plasma nucleic acid are disturbed in ALS patients, which may link to the abnormal DNA damage or RNA metabolism.

Pathologically, the toxic protein aggregation in the cytoplasm is the prominent feature in ALS, and the abnormal metabolism of amino acids could be correlated with the development of ALS. The SERS spectroscopy could detect several kinds of amino acids in the blood plasma, including arginine (band at 493 cm^{-1}), tyrosine (band at 635 and 1618 cm^{-1}), tryptophan (band at 760 , 1198 , and 1618 cm^{-1}), L-Serine (band at 808 cm^{-1}), and phenylalanine (band at 1001 and 1198 cm^{-1}). Hżeczka et al. explored the plasma amino acid percentages in ALS patients and controls, and they observed that the percentages of tyrosine, valine, methionine, leucine, and isoleucine were lower, while the percentages of glutamine and serine were higher in ALS than in controls.²³ In the present study, we also observed that the intensity of tyrosine

(band at 635 cm^{-1}) was lower in ALS than in controls. In the aspect of pathway analysis, Patin et al. highlighted that arginine-proline, tryptophan, and branched amino acid metabolic pathways were associated with ALS evolution.²⁴ In this study, we also identified several amino acid metabolism-related pathways, including phenylalanine-tyrosine-tryptophan biosynthesis, aminoacyl-tRNA biosynthesis, and phenylalanine metabolism. The mechanisms underlying the disturbed amino acid metabolisms to ALS still need further investigations.

To explore the diagnostic role of plasma SERS spectrum in ALS, we constructed DT models to perform CRT analysis for ALS-1 and control, ALS-2 and control, and ALS-3 and control, respectively, and identified some important SERS bands. We then evaluated the predictive performance of each SERS band by ROC curve. The band of 722 and 739 cm^{-1} showed better predictive performance with the largest AUC. We also explored the ratio of different SERS bands, and it indicated that the ratio of $635\text{--}722\text{ cm}^{-1}$, and ratio of $635\text{--}739\text{ cm}^{-1}$ possessed the best predictive performance. For a suspected ALS patient, it could be useful to perform blood plasma SERS analysis, and the bands of 722 and 739 cm^{-1} , as well as the ratio of $635\text{--}722\text{ cm}^{-1}$, and $635\text{--}739\text{ cm}^{-1}$ could be helpful to confirm the diagnosis of ALS. Previously, we also compared the SERS spectral features of ALS patients between the fast and slow progression groups, and it possessed the capability to distinguish the ALS patients with high sensitivity and specificity, which provided a clue that plasma SERS could also serve as a tool for disease severity and prognosis prediction.⁸ Additionally, we also noted several limitations in our study. There are a few SERS bands that

cannot be assigned to compounds at present, such as the band at 1385 cm^{-1} corresponds to C–H rocking, and the band intensity was higher in ALS than in controls. Besides, only 5–10% of ALS patients are familial, and we enrolled 12 inherited cases in the present study. Due to a small number of familial cases, we have not analyzed separately. Finally, it is necessary to compare the plasma SERS spectra between ALS and other patients with neurological disorders, such as stroke, dementia, spinal muscular atrophy, hereditary spastic paraplegia, and peripheral neuropathy, aiming to further clarify the specificity of SERS spectra in ALS.

Acknowledgments

The authors sincerely thank the ALS patients for their help and willingness to participate in this study. We also thank Steven Boeynaems, PhD, from Department of Genetics, School of Medicine, Stanford University, for editing the English text of a draft of this manuscript. This work was supported by the National Natural Science Foundation of China (grant No. 81701133 and 61975031), the Joint Funds for the Innovation of Science and Technology, Fujian Province (grant No. 2017Y9087), the Distinguished Young Scientific Research Talents Plan in Universities of Fujian Province (grant No. 2018B036), the Scientific Research Talent Training Project of Fujian Provincial Health and Family Planning Commission (grant No. 2018-1-70), and National Key Clinical Specialty Discipline Construction Program and Key Clinical Specialty Discipline Construction Program of Fujian.

Conflict of Interest

None.

Author Contributions

Study concept and design: Drs N Wang, S-Y Feng, and Q-J Zhang; acquisition and interpretation of data: Drs Q-J Zhang, Y Chen, X-H Zou, W Hu, M-L Ye, Q-F Guo and X-L Lin; drafting of the manuscript: Drs Q-J Zhang and Y Chen; critical revision of the manuscript for important intellectual content: Drs N Wang, S-Y Feng and Q-J Zhang; obtaining of funding: Drs Q-J Zhang, Y Chen, S-Y Feng and N Wang; study supervision: Drs Q-J Zhang, S-Y Feng and N Wang.

References

1. van Es MA, Hardiman O, Chio A, et al. Amyotrophic lateral sclerosis. *Lancet* 2017;390:2084–2098.

2. Xu L, Liu T, Liu L, et al. Global variation in prevalence and incidence of amyotrophic lateral sclerosis: a systematic review and meta-analysis. *J Neurol* 2020;267:944–953.
3. Renton AE, Chiò A, Traynor BJ. State of play in amyotrophic lateral sclerosis genetics. *Nat Neurosci* 2014;17:17–23.
4. Liu ZJ, Lin HX, Wei Q, et al. Genetic spectrum and variability in Chinese patients with amyotrophic lateral sclerosis. *Aging Dis* 2019;10:1199–1206.
5. Brown RH, Al-Chalabi A. Amyotrophic lateral sclerosis. *N Engl J Med* 2017;377:162–172.
6. Kneipp J, Kneipp H, Kneipp K. SERS—a single-molecule and nanoscale tool for bioanalytics. *Chem Soc Rev* 2008;37:1052–1060.
7. Kong K, Kendall C, Stone N, Nottingher I. Raman spectroscopy for medical diagnostics—From in-vitro biofluid assays to in-vivo cancer detection. *Adv Drug Deliv Rev* 2015;89:121–134.
8. Zhang QJ, Chen Y, Zou XH, et al. Prognostic analysis of amyotrophic lateral sclerosis based on clinical features and plasma surface-enhanced Raman spectroscopy. *J Biophotonics*. 2019;12:e201900012. <https://doi.org/10.1002/jbio.201900012>
9. Carlomagno C, Banfi PI, Gualerzi A, et al. Human salivary Raman fingerprint as biomarker for the diagnosis of Amyotrophic Lateral Sclerosis. *Sci Rep* 2020;10:10175. <https://doi.org/10.1038/s41598-020-67138-8>
10. Brooks BR, Miller RG, Swash M, Munsat TL; World Federation of Neurology Research Group on Motor Neuron Diseases. El Escorial revisited: revised criteria for the diagnosis of amyotrophic lateral sclerosis. *Amyotroph Lateral Scler Other Motor Neuron Disord* 2000;1:293–299.
11. Leopold N, Lendl B. A new method for fast preparation of highly surface-enhanced Raman scattering (SERS) active silver colloids at room temperature by reduction of silver nitrate with hydroxylamine hydrochloride. *J Phys Chem B* 2003;107:5723–5727.
12. Zhao J, Lui H, McLean DI, Zeng H. Automated autofluorescence background subtraction algorithm for biomedical Raman spectroscopy. *Appl Spectrosc* 2007;61:1225–1232.
13. Bonifacio A, Dalla Marta S, Spizzo R, et al. Surface-enhanced Raman spectroscopy of blood plasma and serum using Ag and Au nanoparticles: a systematic study. *Anal Bioanal Chem* 2014;406:2355–2365.
14. Feng S, Wang W, Tai IT, et al. Label-free surface-enhanced Raman spectroscopy for detection of colorectal cancer and precursor lesions using blood plasma. *Biomed Opt Express* 2015;6:3494–3502.
15. Orsagova Kralova Z, Orinak A, Orinakova R, et al. Electrochemically deposited silver detection substrate for surface-enhanced Raman spectroscopy cancer diagnostics. *J Biomed Opt* 2018;23:1–11.

16. Rothstein JD. Current hypotheses for the underlying biology of amyotrophic lateral sclerosis. *Ann Neurol* 2009;65(Suppl 1):S3–S9.
17. Turner MR, Hardiman O, Benatar M, et al. Controversies and priorities in amyotrophic lateral sclerosis. *Lancet Neurol* 2013;12:310–322.
18. Zhao M, Kim JR, van Bruggen R, Park J. RNA-binding proteins in amyotrophic lateral sclerosis. *Mol Cells* 2018;4:818–829.
19. Ellis DI, Goodacre R. Metabolic fingerprinting in disease diagnosis: biomedical applications of infrared and Raman spectroscopy. *Analyst* 2006;131:875–885.
20. Martin LJ. DNA damage and repair: relevance to mechanisms of neurodegeneration. *J Neuropathol Exp Neurol* 2008;67:377–387.
21. Kim BW, Jeong YE, Wong M, Martin LJ. DNA damage accumulates and responses are engaged in human ALS brain and spinal motor neurons and DNA repair is activatable in iPSC-derived motor neurons with SOD1 mutations. *Acta Neuropathol Commun* 2020;8:7. <https://doi.org/10.1186/s40478-019-0874-4>
22. Baradaran-Heravi Y, Van Broeckhoven C, van der Zee J. Stress granule mediated protein aggregation and underlying gene defects in the FTD-ALS spectrum. *Neurobiol Dis* 2019;134:104639. <https://doi.org/10.1016/j.nbd.2019.104639>
23. Ilzecka J, Stelmasiak Z, Solski J, et al. Plasma amino acids percentages in amyotrophic lateral sclerosis patients. *Neurol Sci* 2003;24:293–295.
24. Patin F, Corcia P, Vourc'h P, et al. Omics to explore amyotrophic lateral sclerosis evolution: the central role of arginine and proline metabolism. *Mol Neurobiol* 2017;54:5361–5374.

Supporting Information

Additional supporting information may be found online in the Supporting Information section at the end of the article.

Figure S1. The intensity distribution and ROC curves for ALS-1, ALS-2, and ALS-3 of band at 493, 529, 587, and 635 cm^{-1} .

Figure S2. The intensity distribution and ROC curves for ALS-1, ALS-2, and ALS-3 of band at 681, 722, 739, and 760 cm^{-1} .

Figure S3. The intensity distribution and ROC curves for ALS-1, ALS-2, and ALS-3 of band at 808, 882, 1001, and 1068 cm^{-1} .

Figure S4. The intensity distribution and ROC curves for ALS-1, ALS-2, and ALS-3 of band at 1130, 1198, 1252, and 1275 cm^{-1} .

Figure S5. The intensity distribution and ROC curves for ALS-1, ALS-2, and ALS-3 of band at 1322, 1385, 1450, and 1507 cm^{-1} .

Figure S6. The intensity distribution and ROC curves for ALS-1, ALS-2, and ALS-3 of band at 1567, 1618, and 1648 cm^{-1} .

Figure S7. The intensity distribution and ROC curves for ALS-1, ALS-2, and ALS-3 of ratio of 529–722 cm^{-1} , 635–722 cm^{-1} , 529–739 cm^{-1} , and 635–739 cm^{-1} .

Figure S8. Map of disease-related metabolic network based on Kyoto Encyclopedia of Genes and Genomes (KEGG) online database. The squares in gray represent the compounds identified in the present study.